SFB F68
Tomography Across the Scales

Technische Universität Berlin

Motion Detection in Diffraction Tomography

Michael Quellmalz | TU Berlin | IPMS Conference, Malta, 28 May 2024
joint work with Robert Beinert, Peter Elbau, Clemens Kirisits, Monika Ritsch-Marte, Otmar Scherzer, Eric Setterqvist, Gabriele Steidl

Outline

Optical Diffraction Tomography (ODT)

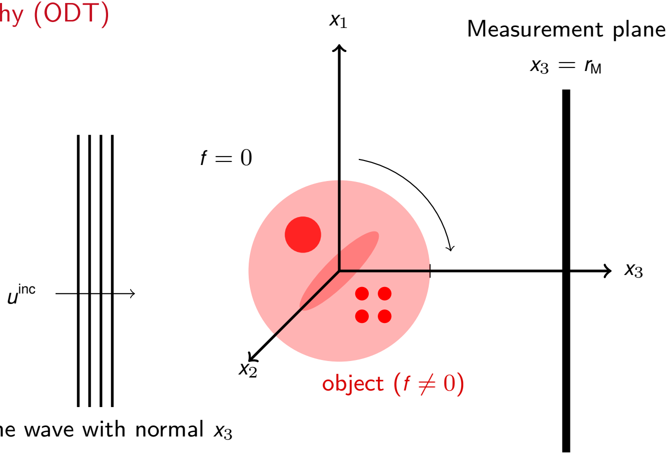

Incident field: Plane wave with normal x_3

Model of Optical Diffraction Tomography (for one direction)

- We have: field $u^{\text{tot}}(\tilde{\boldsymbol{x}}, r_M)$, $\tilde{\boldsymbol{x}} \in \mathbb{R}^{d-1}$, at measurement plane $x_d = r_M$
- We want: scattering potential f on $\mathbb{R}^d$ with compact support
- Illumination by plane wave $u^{\text{inc}}(\boldsymbol{x}) = e^{ik_0 \boldsymbol{x}\cdot\boldsymbol{s}}$ with direction $\boldsymbol{s} \in \mathbb{S}^{d-1}$ and wave number k_0
- Total field $u^{\text{tot}}(\boldsymbol{x}) = u(\boldsymbol{x}) + u^{\text{inc}}(\boldsymbol{x})$ solves the wave equation

$$-\left(\Delta + f(\boldsymbol{x}) + k_0^2\right) u^{\text{tot}}(\boldsymbol{x}) = 0$$

- Rearranging yields

$$-\left(\Delta + k_0^2\right) u(\boldsymbol{x}) - \underbrace{\left(\Delta + k_0^2\right) u^{\text{inc}}(\boldsymbol{x})}_{=0} = f(\boldsymbol{x}) \left(u(\boldsymbol{x}) + u^{\text{inc}}(\boldsymbol{x})\right)$$

Born approximation

Assuming $|u| \ll |u^{\text{inc}}|$, we obtain

$$-\left(\Delta + k_0^2\right) u(\boldsymbol{x}) = f(\boldsymbol{x}) u^{\text{inc}}(\boldsymbol{x}) \tag{1}$$

Model of Optical Diffraction Tomography (for one direction)

- We have: field $u^{\mathrm{tot}}(\tilde{\boldsymbol{x}}, r_{\mathrm{M}})$, $\tilde{\boldsymbol{x}} \in \mathbb{R}^{d-1}$, at measurement plane $x_d = r_{\mathrm{M}}$
- We want: scattering potential f on $\mathbb{R}^d$ with compact support
- Illumination by plane wave $u^{\mathrm{inc}}(\boldsymbol{x}) = \mathrm{e}^{\mathrm{i}k_0 \boldsymbol{x}\cdot\boldsymbol{s}}$ with direction $\boldsymbol{s} \in \mathbb{S}^{d-1}$ and wave number k_0
- Total field $u^{\mathrm{tot}}(\boldsymbol{x}) = u(\boldsymbol{x}) + u^{\mathrm{inc}}(\boldsymbol{x})$ solves the wave equation

$$-\left(\Delta + f(\boldsymbol{x}) + k_0^2\right) u^{\mathrm{tot}}(\boldsymbol{x}) = 0$$

- Rearranging yields

$$-\left(\Delta + k_0^2\right) u(\boldsymbol{x}) - \underbrace{\left(\Delta + k_0^2\right) u^{\mathrm{inc}}(\boldsymbol{x})}_{=0} = f(\boldsymbol{x}) \left(u(\boldsymbol{x}) + u^{\mathrm{inc}}(\boldsymbol{x})\right)$$

Born approximation

Assuming $|u| \ll |u^{\mathrm{inc}}|$, we obtain

$$-\left(\Delta + k_0^2\right) u(\boldsymbol{x}) = f(\boldsymbol{x}) u^{\mathrm{inc}}(\boldsymbol{x}) \qquad (1)$$

Model of Optical Diffraction Tomography (for one direction)

- We have: field $u^{\text{tot}}(\tilde{\boldsymbol{x}}, r_{\text{M}})$, $\tilde{\boldsymbol{x}} \in \mathbb{R}^{d-1}$, at measurement plane $x_d = r_{\text{M}}$
- We want: scattering potential f on $\mathbb{R}^d$ with compact support
- Illumination by plane wave $u^{\text{inc}}(\boldsymbol{x}) = \mathrm{e}^{\mathrm{i}k_0 \boldsymbol{x}\cdot\boldsymbol{s}}$ with direction $\boldsymbol{s} \in \mathbb{S}^{d-1}$ and wave number k_0
- Total field $u^{\text{tot}}(\boldsymbol{x}) = u(\boldsymbol{x}) + u^{\text{inc}}(\boldsymbol{x})$ solves the wave equation

$$-\left(\Delta + f(\boldsymbol{x}) + k_0^2\right) u^{\text{tot}}(\boldsymbol{x}) = 0$$

- Rearranging yields

$$-\left(\Delta + k_0^2\right) u(\boldsymbol{x}) - \underbrace{\left(\Delta + k_0^2\right) u^{\text{inc}}(\boldsymbol{x})}_{=0} = f(\boldsymbol{x})\left(u(\boldsymbol{x}) + u^{\text{inc}}(\boldsymbol{x})\right)$$

Born approximation

Assuming $|u| \ll |u^{\text{inc}}|$, we obtain

$$-\left(\Delta + k_0^2\right) u(\boldsymbol{x}) = f(\boldsymbol{x}) u^{\text{inc}}(\boldsymbol{x}) \tag{1}$$

Lemma

For $g \in L^1(\mathbb{R}^d)$ with compact support,

$$u = g * G \in L^1_{\mathrm{loc}}(\mathbb{R}^d) \cap \mathcal{S}'(\mathbb{R}^d)$$

is the unique outgoing solution of the Helmholtz equation (1), with fundamental solution

$$G(\boldsymbol{x}) = \frac{\mathrm{i}}{4} \left(\frac{k_0}{2\pi |\boldsymbol{x}|} \right)^{\frac{d-2}{2}} H^{(1)}_{\frac{d-2}{2}}(k_0 |\boldsymbol{x}|),$$

where $H^{(1)}_a$ is the Hankel function of the first kind and order a.

Lemma

If $g_n \to 0$ in $L^1(\mathbb{R}^d)$ and $\bigcup_n \operatorname{supp} g_n$ is bounded, then $g_n * G \to 0$ in $\mathcal{S}'(\mathbb{R}^d)$.

Fourier diffraction theorem

Let

- u be the outgoing solution of the Helmholtz equation (1),
- $f \in L^1(\mathbb{R}^d)$ have compact support,
- the incident field $u^{\mathrm{inc}}(\boldsymbol{x}) = \mathrm{e}^{\mathrm{i}k_0 \boldsymbol{x}\cdot\boldsymbol{s}}$, and
- the measurement plane $x_d = r_M$ not intersect $\operatorname{supp} f$.

Then

$$\sqrt{\frac{2}{\pi}}\kappa \mathrm{i}\mathrm{e}^{-\mathrm{i}\kappa r_M}\tilde{\mathcal{F}}\underbrace{u(\tilde{\boldsymbol{x}}, r_M)}_{\text{measured}} = \mathcal{F}f(\boldsymbol{h}(\tilde{\boldsymbol{x}}) - k_0\boldsymbol{s}), \quad \tilde{\boldsymbol{x}} \in \mathbb{R}^{d-1},$$

where $\tilde{\mathcal{F}}$ is the Fourier transform in $d-1$ coordinates, $\boldsymbol{h}(\tilde{\boldsymbol{x}}) := \begin{pmatrix} \tilde{\boldsymbol{x}} \\ \kappa \end{pmatrix}$ and $\kappa := \sqrt{k_0^2 - |\tilde{\boldsymbol{x}}|^2}$.

based on [Wolf 1969] [Natterer Wuebbeling 2001] [Kak Slaney 2001]
this L^p version from [Kirisits Q. Setterqvist 2024]

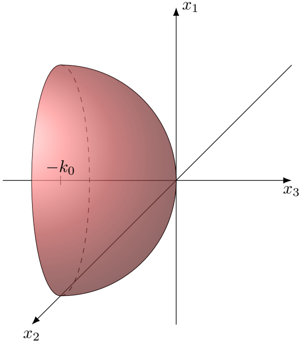

Semisphere $\boldsymbol{h}(\boldsymbol{k})$ of available data in Fourier space

Rigid Motion of the Object

- Scattering potential of the moved object: $f(R_t(\boldsymbol{x} - \boldsymbol{d}_t))$
- Rotation $R_t \in \mathrm{SO}(d)$ (with $R_0 := \mathrm{id}$)
- Translation $\boldsymbol{d}_t \in \mathbb{R}^d$ (with $\boldsymbol{d}_0 := \mathbf{0}$)
- Incidence direction $\boldsymbol{s}_t \in \mathbb{S}^{d-1}$

Fourier diffraction theorem (with motion)

The quantity

$$\mu_t(\boldsymbol{x}) := \sqrt{\frac{2}{\pi}}\kappa \mathrm{i} \mathrm{e}^{-\mathrm{i}\kappa r_{\mathrm{M}}} \tilde{\mathcal{F}} u(\boldsymbol{k}, r_{\mathrm{M}}) = \mathcal{F} f(\underbrace{R_t \boldsymbol{h}(\boldsymbol{x}) - k_0 \boldsymbol{s}_t}_{\text{Fourier cover}})\, \mathrm{e}^{-\mathrm{i}\langle \boldsymbol{d}_t, \boldsymbol{h}(\boldsymbol{x})\rangle}, \quad \|\boldsymbol{x}\| < k_0,$$

depends only on the measurements.

Fourier cover: Angle scan

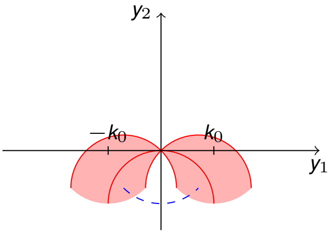

Quarter turn $t \in [\pi/4, 3\pi/4]$

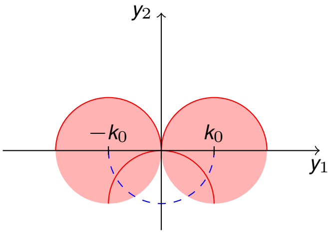

Half turn $t \in [0, \pi]$

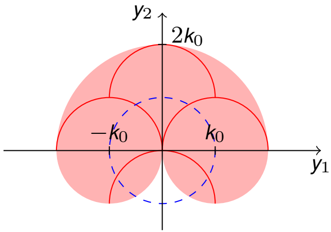

Full turn $t \in [0, 2\pi]$

2D Fourier coverage for incidence direction $\boldsymbol{s}(t) = (\cos t, \sin t)$. Measurements are taken at $r_2 = r_M$. The Fourier coverage (light red) is a union of infinitely many semicircles, whose centers lie on the dashed blue curve.

Fourier cover: Object rotation

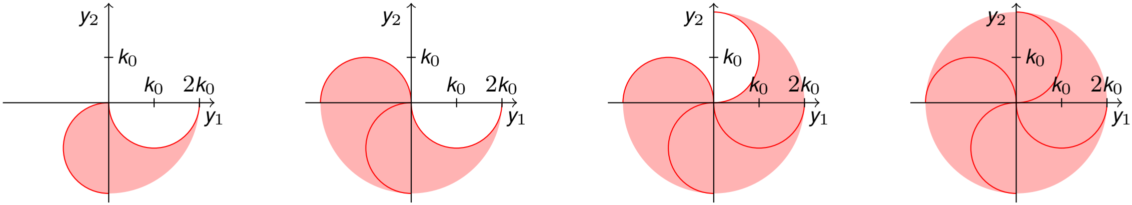

(a) Quarter turn (b) Half turn (c) Three-quarter turn (d) Full turn

Figure: 2D Fourier coverage for a rotating object, incidence direction $\boldsymbol{s} = (1, 0)$ and measurements taken at $r_2 = r_M$.

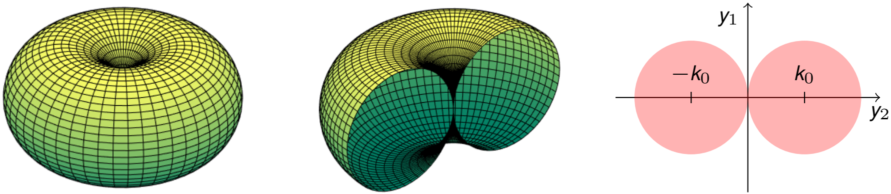

Figure: 3D Fourier coverage for a full rotation of the object about the r_1-axis with incidence direction $\boldsymbol{s} = (0, 1, 0)$.

Fourier cover: Angle scan & Rotation

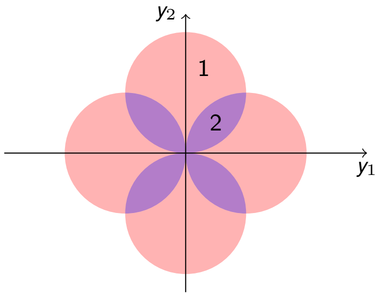

2D Fourier cover
(colors represent Banch indicatrix)

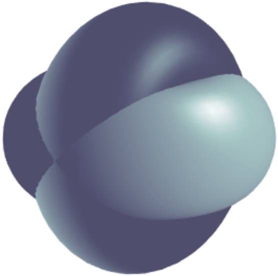

3D Fourier cover

- Incidence is rotated along a half circle
- and the experiment is repeated with the object rotated by 90°.

Outline

Filtered Backpropagation

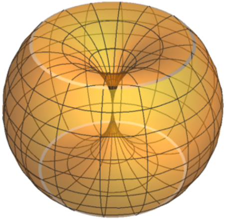

Idea: Inverse Fourier transform of $\mathcal{F}f$ restricted to the set of available data $\mathcal{Y}$,

$$f_{\mathrm{bp}}(\boldsymbol{r}) := (2\pi)^{-\frac{d}{2}} \int_{\mathcal{Y}} \mathcal{F}f(\boldsymbol{y})\, \mathrm{e}^{\mathrm{i}\boldsymbol{y}\cdot\boldsymbol{r}}\, \mathrm{d}\boldsymbol{y}$$

with the transformation $T(\boldsymbol{x}, t) := R_t \boldsymbol{h}(\boldsymbol{x})$

Theorem [Kirisits, Q, Setterqvist 2024]

Let the rotation $R_t \in SO(d)$, translation $\boldsymbol{d}_t$ and incidence $\boldsymbol{s}_t \in \mathbb{S}^{d-1}$ be piecewice C^1. Then

$$f_{\mathrm{bp}}(\boldsymbol{r}) = (2\pi)^{-\frac{d}{2}} \int_0^T \int_{\mathcal{B}_{k_0}} \mathcal{F}f(T(\boldsymbol{x}, t))\, \mathrm{e}^{\mathrm{i}\, T(\boldsymbol{x},t)\cdot(\boldsymbol{r}+\boldsymbol{d}_t)} \frac{|\det \nabla T(\boldsymbol{x}, t)|}{\operatorname{Card} T^{-1}(T(\boldsymbol{x}, t))}\, \mathrm{d}\boldsymbol{x}\, \mathrm{d}t,$$

where $\det \nabla T(\boldsymbol{x}, t) = \dfrac{k_0(t)k_0'(t) - R_t\boldsymbol{h}(\boldsymbol{x}, t)\,(k_0(t)R_t\boldsymbol{s}_t)'}{\kappa}$.

Banach indicatrix $\operatorname{Card}(T^{-1}(\boldsymbol{y}))$ needs to be estimated (except for special cases).
Well-known for rotation around coordinate axis [Devaney 1982]

Filtered Backpropagation

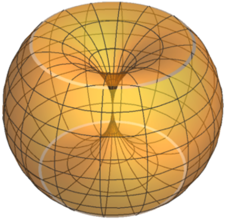

Idea: Inverse Fourier transform of $\mathcal{F}f$ restricted to the set of available data $\mathcal{Y}$,

$$f_{\mathrm{bp}}(\boldsymbol{r}) := (2\pi)^{-\frac{d}{2}} \int_{\mathcal{Y}} \mathcal{F}f(\boldsymbol{y})\, \mathrm{e}^{\mathrm{i}\boldsymbol{y}\cdot\boldsymbol{r}}\, \mathrm{d}\boldsymbol{y}$$

with the transformation $T(\boldsymbol{x}, t) := R_t \boldsymbol{h}(\boldsymbol{x})$

Theorem [Kirisits, Q, Setterqvist 2024]

Let the rotation $R_t \in SO(d)$, translation $\boldsymbol{d}_t$ and incidence $\boldsymbol{s}_t \in \mathbb{S}^{d-1}$ be piecewice C^1. Then

$$f_{\mathrm{bp}}(\boldsymbol{r}) = (2\pi)^{-\frac{d}{2}} \int_0^T \int_{\mathcal{B}_{k_0}} \mathcal{F}f(T(\boldsymbol{x}, t))\, \mathrm{e}^{\mathrm{i}\, T(\boldsymbol{x},t)\cdot(\boldsymbol{r}+\boldsymbol{d}_t)} \frac{|\det \nabla T(\boldsymbol{x}, t)|}{\mathrm{Card}\, T^{-1}(T(\boldsymbol{x}, t))}\, \mathrm{d}\boldsymbol{x}\, \mathrm{d}t,$$

where $\det \nabla T(\boldsymbol{x}, t) = \dfrac{k_0(t)k_0'(t) - R_t\boldsymbol{h}(\boldsymbol{x}, t)\,(k_0(t)R_t\boldsymbol{s}_t)'}{\kappa}$.

Banach indicatrix $\mathrm{Card}(T^{-1}(\boldsymbol{y}))$ needs to be estimated (except for special cases).
Well-known for rotation around coordinate axis [Devaney 1982]

Discretization

- Object $f(\boldsymbol{x_k})$ with $\boldsymbol{x_k} = \boldsymbol{k}\frac{2L_s}{K}$, $\boldsymbol{k} \in \mathcal{I}_K^3 := \{-K/2, \dots, K/2-1\}^3$
- Measurements $u_{t_m}^{\mathrm{tot}}(\boldsymbol{y_n}, r_M)$ with $\boldsymbol{y_n} = \boldsymbol{n}\frac{2L_M}{N}$, $\boldsymbol{n} \in \mathcal{I}_N^2$
- discrete Fourier transform (DFT)

$$[\boldsymbol{F}_{\mathrm{DFT}}\, u_{t_m}]_{\boldsymbol{\ell}} := \sum_{\boldsymbol{n}\in\mathcal{I}_N^2} u_{t_m}(\boldsymbol{y_n}, r_M)\, \mathrm{e}^{-2\pi \mathrm{i} \boldsymbol{n}\cdot\boldsymbol{\ell}/N}, \qquad \boldsymbol{\ell} \in \mathcal{I}_N^2,$$

- Non-uniform discrete Fourier transform (NDFT)

$$[\boldsymbol{F}_{\mathrm{NDFT}}\boldsymbol{f}]_{m,\boldsymbol{\ell}} := \sum_{\boldsymbol{k}\in\mathcal{I}_K^3} f_{\boldsymbol{k}}\, \mathrm{e}^{-\mathrm{i}\boldsymbol{x_k}\cdot\left(R_{t_m}\boldsymbol{h}(\boldsymbol{y_\ell})\right)}, \qquad m \in \mathcal{J}_M,\ \boldsymbol{\ell} \in \mathcal{I}_N^2$$

Discretized forward operator

$$\boldsymbol{D}^{\mathrm{tot}}\boldsymbol{f} := \boldsymbol{F}_{\mathrm{DFT}}^{-1}(\boldsymbol{c} \odot \boldsymbol{F}_{\mathrm{NDFT}}\boldsymbol{f}) + \mathrm{e}^{\mathrm{i}k_0 r_M}, \qquad \boldsymbol{f} \in \mathbb{R}^{K^d},$$

where $\boldsymbol{c} = \left[\frac{\mathrm{i}}{\kappa(\boldsymbol{y_\ell})}\, \mathrm{e}^{\mathrm{i}\,\kappa(\boldsymbol{y_\ell})\, r_M} \left(\frac{N}{L_M}\right)^{d-1} \left(\frac{L_s}{K}\right)^{d}\right]_{\boldsymbol{\ell}\in\mathcal{I}_N^2}$

Reconstruction of f

Inverse

$$\boldsymbol{f} \approx \boldsymbol{F}_{\text{NDFT}}^{-1}\left(\left(\boldsymbol{F}_{\text{DFT}}\boldsymbol{u}^{\text{tot}} - e^{ik_0 r_{\text{M}}}\right) \oslash \boldsymbol{c}\right)$$

Crucial part: inversion of NDFT $\boldsymbol{F}_{\text{NDFT}}^{-1}$

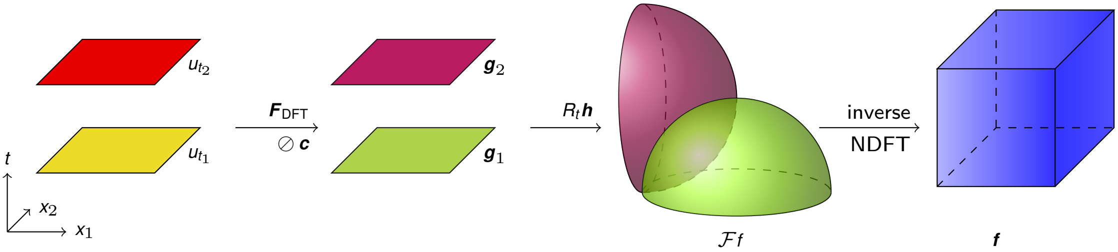

Conjugate Gradient (CG) Method

- Conjugate Gradients (CG) on the normal equations

$$\operatorname*{arg\,min}_{\boldsymbol{f}\in\mathbb{R}^{K^3}} \quad \|\boldsymbol{F}_{\mathrm{NDFT}}(\boldsymbol{f}) - \boldsymbol{g}\|_2^2$$

- NFFT (Non-uniform fast Fourier transform) for computing $\boldsymbol{F}_{\mathrm{NDFT}}(\boldsymbol{f})$ in $\mathcal{O}\left(N^3 \log N\right)$ steps

[Dutt Rokhlin 93], [Beylkin 95], [Potts Steidl Tasche 01], [Potts Kunis Keiner 04+]

TV (Total Variation) Regularization

- Regularized inverse

$$\operatorname*{arg\,min}_{\boldsymbol{f}\in\mathbb{R}^{K^3}} \quad \chi_{\mathbb{R}^{K^3}_{\geq 0}}(\boldsymbol{f}) + \frac{1}{2}\|\boldsymbol{F}_{\mathrm{NDFT}}(\boldsymbol{f}) - \boldsymbol{g}\|_2^2 + \lambda \mathrm{TV}(\boldsymbol{f}),$$

- Primal-dual (PD) iteration [Chambolle & Pock 2010]
- Adaptive selection of step sizes [Yokota & Hontani 2017]

Conjugate Gradient (CG) Method

- Conjugate Gradients (CG) on the normal equations

$$\underset{\boldsymbol{f}\in\mathbb{R}^{K^3}}{\arg\min} \quad \|\boldsymbol{F}_{\mathrm{NDFT}}(\boldsymbol{f}) - \boldsymbol{g}\|_2^2$$

- NFFT (Non-uniform fast Fourier transform) for computing $\boldsymbol{F}_{\mathrm{NDFT}}(\boldsymbol{f})$ in $\mathcal{O}\left(N^3 \log N\right)$ steps

[Dutt Rokhlin 93], [Beylkin 95], [Potts Steidl Tasche 01], [Potts Kunis Keiner 04+]

TV (Total Variation) Regularization

- Regularized inverse

$$\underset{\boldsymbol{f}\in\mathbb{R}^{K^3}}{\arg\min} \quad \chi_{\mathbb{R}^{K^3}_{\geq 0}}(\boldsymbol{f}) + \frac{1}{2}\|\boldsymbol{F}_{\mathrm{NDFT}}(\boldsymbol{f}) - \boldsymbol{g}\|_2^2 + \lambda \mathrm{TV}(\boldsymbol{f}),$$

- Primal-dual (PD) iteration [Chambolle & Pock 2010]
- Adaptive selection of step sizes [Yokota & Hontani 2017]

Reconstruction: Moving Rotation Axis

Ground truth ***f***
($240 \times 240 \times 240$ grid)

Backpropagation
PSNR 24.17
SSIM 0.171
5 s

Backpropagation
(with inticatrix estimation)
PSNR 31.84
SSIM 0.350
5 s +22 s precopmpute

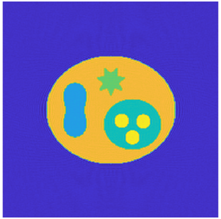

CG Reconstruction
PSNR 35.84
SSIM 0.962
82 s

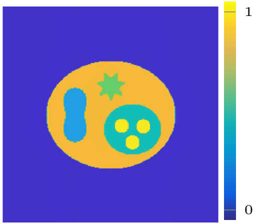

TV ($\lambda = 0.02$)
PSNR 40.95
SSIM 0.972
1395 s

Reconstruction: Moving Rotation Axis and 5 % Gaussian Noise

Ground truth ***f***

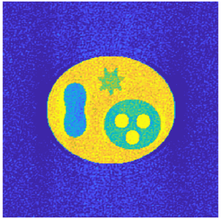

Backpropagation
PSNR 21.19
SSIM 0.075

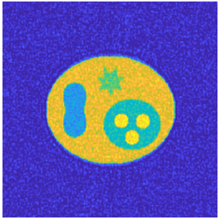

Backpropagation (with indicatrix estimation)
PSNR 25.50
SSIM 0.157

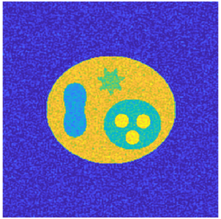

CG Reconstruction
PSNR 24.10
SSIM 0.193

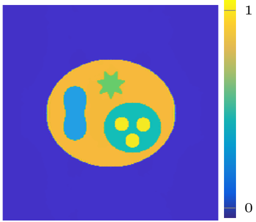

TV ($\lambda = 0.05$)
PSNR 38.01
SSIM 0.772

Outline

1. Introduction
2. Reconstruction of the object
3. **Reconstructing the motion**

Formal Uniqueness Result

Theorem [Kurlberg Zickert 2021]

Let

- the matrix of second-order moments of f have distinct, real eigenvalues,
- certain third-order moments do not vanish,
- the translation $\boldsymbol{d}_t$ be restricted to a known plane,
- the rotations R_t cover $\mathrm{SO}(3)$.

Then f is uniquely determined given the diffraction images u_t for all (unknown) motions.

We find an algorithm to recover the rotations and translations

Detection of the Rotation in 3D

Goal: Estimate the rotation R_t from the transformed measurements $\nu_t(\boldsymbol{k}) = |\mathcal{F}f(R_t\boldsymbol{h}(\boldsymbol{k}))|^2$

Common circle approach:

- For each t we have the Fourier data $\mathcal{F}f$ on one semisphere
- Two semispheres intersect in a circle (arc), where $\mathcal{F}f$ must agree
- Find the common circle of two semispheres

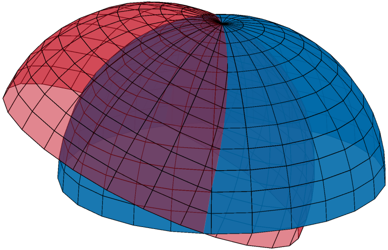

Dual Common Circles

- f real-valued (no absorption)
- Additional symmetry $\mathcal{F}f(\boldsymbol{y}) = \overline{\mathcal{F}f(-\boldsymbol{y})}$
- Additional pair of “dual” common circles

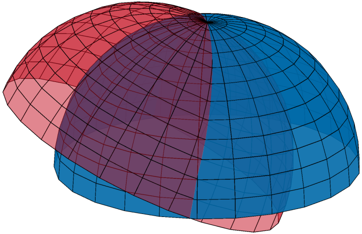

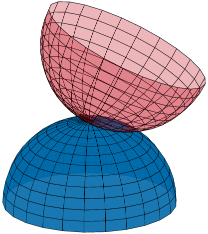

For $\varphi \in [0, 2\pi)$, $\theta \in [0, \pi]$, we can parameterize the common circles in the 2D data by

$$\gamma^{\varphi,\theta}(\beta) := \frac{k_0}{2} \sin(\theta)(\cos(\beta) - 1) \begin{pmatrix} \cos(\varphi) \\ \sin(\varphi) \end{pmatrix} + k_0 \cos(\tfrac{\theta}{2}) \sin(\beta) \begin{pmatrix} -\sin(\varphi) \\ \cos(\varphi) \end{pmatrix}, \quad \beta \in \mathbb{R},$$

$$\check{\gamma}^{\varphi,\theta}(\beta) := -\frac{k_0}{2} \sin(\theta)(\cos(\beta) - 1) \begin{pmatrix} \cos(\varphi) \\ \sin(\varphi) \end{pmatrix} - k_0 \sin(\tfrac{\theta}{2}) \sin(\beta) \begin{pmatrix} -\sin(\varphi) \\ \cos(\varphi) \end{pmatrix}, \quad \beta \in \mathbb{R}.$$

Theorem (unique reconstruction) [Q. Elbau Scherzer Steidl 2024]

Let $s, t \in [0, T]$. Assume that there exist unique angles $\varphi, \psi \in \mathbb{R}/(2\pi\mathbb{Z})$ and $\theta \in [0, \pi]$ such that

$$\nu_s(\gamma^{\varphi,\theta}(\beta)) = \nu_t(\gamma^{\pi-\psi,\theta}(-\beta)) \quad \forall \beta \in [-\tfrac{\pi}{2}, \tfrac{\pi}{2}] \quad \text{and}$$

$$\nu_s(\check{\gamma}^{\varphi,\theta}(\beta)) = \nu_t(\check{\gamma}^{\pi-\psi,\theta}(\beta)) \quad \forall \beta \in [-\tfrac{\pi}{2}, \tfrac{\pi}{2}].$$

Then the relative rotation $R_s^\top R_t$ is uniquely determined by the Euler angles

$$R_s^\top R_t = Q^{(3)}(\varphi)\, Q^{(2)}(\theta)\, Q^{(3)}(\psi),$$

where $Q^{(i)}(\alpha)$ denotes the rotation around the i-th coordinate with angle α.

Visualization of the Common Arcs

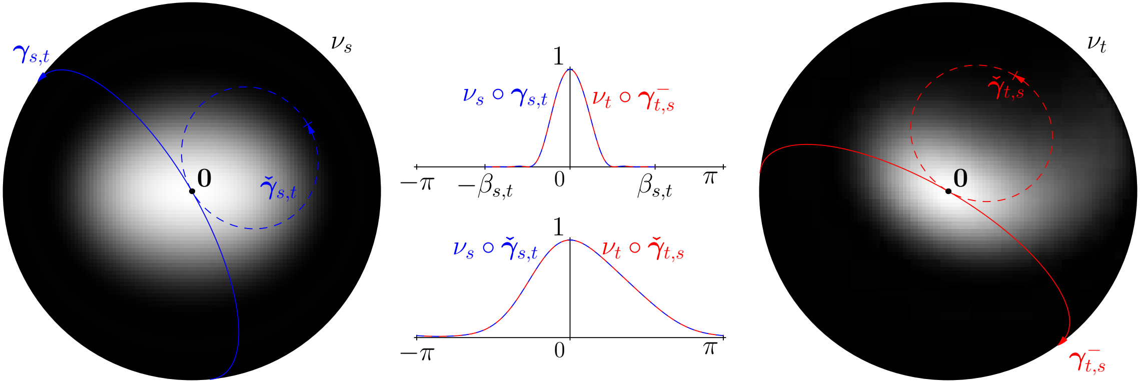

Here $\gamma_{s,t} := \gamma^{\varphi,\theta}$ and $\gamma_{t,s} := \gamma^{\pi-\psi,\theta}$ for $R_s^\top R_t = Q^{(3)}(\varphi)\, Q^{(2)}(\theta)\, Q^{(3)}(\psi)$

Infinitesimal Common Circles Method

Theorem [Q. Elbau Scherzer Steidl 2024]

Let the rotation $R \in C^1([0,T] \to \mathrm{SO}(3))$ and $t \in (0,T)$.
We define the associated **angular velocity** as the vector $\boldsymbol{\omega}_t \in \mathbb{R}^3$ satisfying

$$R_t^\top R_t' \, \boldsymbol{y} = \boldsymbol{\omega}_t \times \boldsymbol{y}, \qquad \boldsymbol{y} \in \mathbb{R}^3,$$

and write it in cylindrical coordinates

$$\boldsymbol{\omega}_t = \begin{pmatrix} \rho\cos\varphi \\ \rho\sin\varphi \\ \zeta \end{pmatrix}.$$

Then

$$-\partial_t \nu_t(r\varphi) = \left(\left(\sqrt{k_0^2 - r^2} - k_0\right)\rho + r\zeta\right) \left\langle \nabla \nu_t(r\varphi), \begin{pmatrix} -\sin\varphi \\ \cos\varphi \end{pmatrix} \right\rangle \qquad \forall r \in (-k_0, k_0).$$

Technische Universität Berlin

Reconstructing the Translation

Recall: Data $\mu_t(\boldsymbol{x}) = \mathcal{F}f(R_t\boldsymbol{h}(\boldsymbol{x}))\,\mathrm{e}^{-\mathrm{i}\langle \boldsymbol{d}_t, \boldsymbol{h}(\boldsymbol{x})\rangle}$

Theorem [Q. Elbau Scherzer Steidl 2024]

Let $s, t \in [0, T]$ be such that $R_s\boldsymbol{e}^3 \neq \pm R_t\boldsymbol{e}^3$. Assume $f \geq 0$, $f \not\equiv 0$ and $\boldsymbol{d}_0 = \mathbf{0}$.
Then $\boldsymbol{d}_t$ can be uniquely reconstructed from the two equations:

$$\mathrm{e}^{\mathrm{i}\left\langle R_t\boldsymbol{d}_t - R_s\boldsymbol{d}_s, R_s\boldsymbol{h}(\gamma_{s,t}(\beta))\right\rangle} = \frac{\mu_s(\gamma_{s,t}(\beta))}{\mu_t(\gamma_{t,s}(-\beta))}, \qquad \beta \in [-\pi, \pi],\ \mu_s(\gamma_{s,t}(\beta)) \neq 0,$$

$$\mathrm{e}^{\mathrm{i}\left\langle R_t\boldsymbol{d}_t - R_s\boldsymbol{d}_s, R_s\boldsymbol{h}(\check{\gamma}_{s,t}(\beta))\right\rangle} = \frac{\overline{\mu_s(\check{\gamma}_{s,t}(\beta))}}{\mu_t(\check{\gamma}_{t,s}(\beta))}, \qquad \beta \in [-\pi, \pi],\ \mu_s(\check{\gamma}_{s,t}(\beta)) \neq 0.$$

Similar reconstruction result for $R_s\boldsymbol{e}^3 = \pm R_t\boldsymbol{e}^3$

Numerical Simulation: Test Functions (3D)

Cell phantom

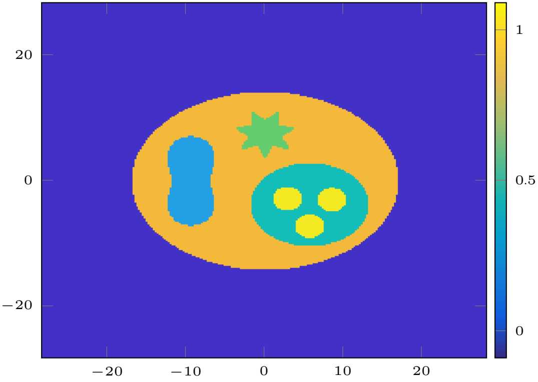

Shepp-Logan phantom

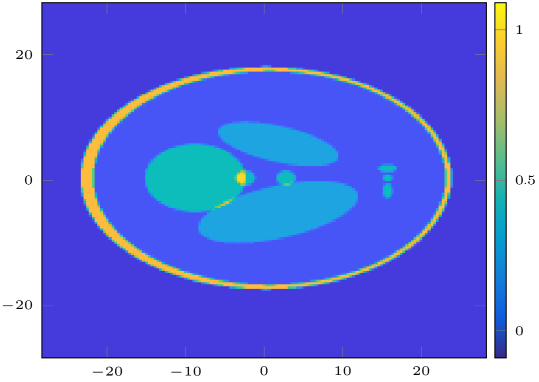

Numerical Simulation: Results

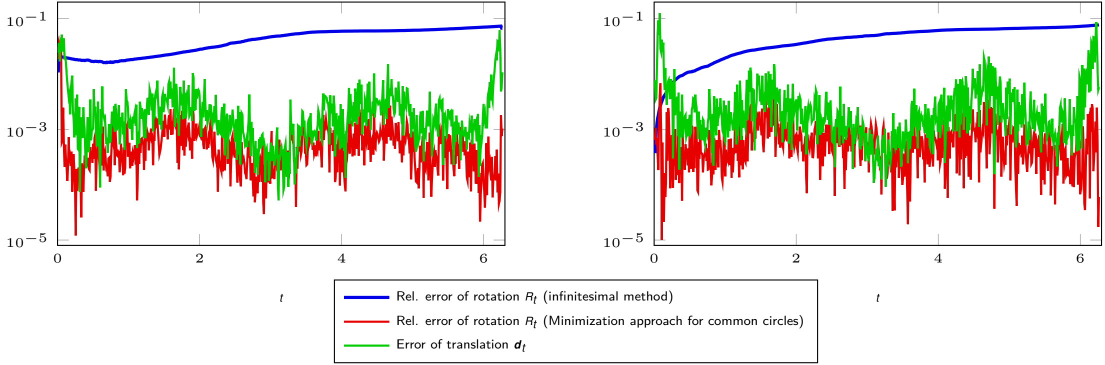

The rotation is around the moving axis $(\sqrt{1-a^2}\cos(b\sin(t/2)), \sqrt{1-a^2}\sin(b\sin(t/2)), a) \in \mathbb{S}^2$ for $a = 0.28$ and $b = 0.5$. The translation is $\boldsymbol{d}_t = 2(\sin t, \sin t, \sin t)$.

Left: cell phantom. Right: Shepp–Logan phantom.

Reconstructed Scattering Potential f

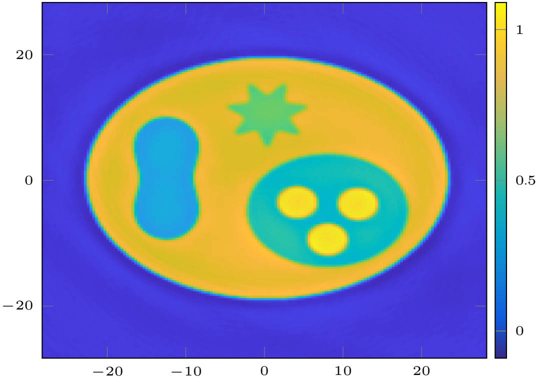

Cell phantom (PSNR 32.21, SSIM 0.754)

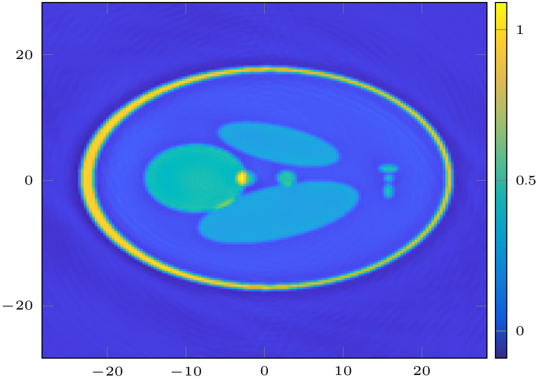

Shepp–Logan (PSNR 30.85, SSIM 0.772)

Conclusions

- Fourier diffraction theorem on $L^1(\mathbb{R}^d)$
- Filtered backpropagation formula for a wide range of experimental setups

- Detection of rotation is mostly possible
- Detection of translation is possible

Future research

- Application to real-world data
- Combining motion detection with phase retrieval

Conclusions

- Fourier diffraction theorem on $L^1(\mathbb{R}^d)$
- Filtered backpropagation formula for a wide range of experimental setups

- Detection of rotation is mostly possible
- Detection of translation is possible

Future research

- Application to real-world data
- Combining motion detection with phase retrieval

References

R. Beinert and M. Quellmalz.
Total variation-based reconstruction and phase retrieval for diffraction tomography.
SIAM Journal on Imaging Sciences, 2022.

R Beinert, M Quellmalz.
Total Variation-Based Reconstruction and Phase Retrieval for Diffraction Tomography with an Arbitrarily Moving Object.
Proceedings in Applied Mathematics & Mechanics 22, 2023. doi:10.1002/pamm.202200135

F. Faucher, C. Kirisits, M. Quellmalz, O. Scherzer, and E. Setterqvist.
Diffraction tomography, Fourier reconstruction, and full waveform inversion.
Handbook of Mathematical Models and Algorithms in Computer Vision and Imaging, pages 273-312. Springer, 2023.

C Kirisits, M Quellmalz, M Ritsch-Marte, O Scherzer, E Setterqvist, G Steidl.
Fourier reconstruction for diffraction tomography of an object rotated into arbitrary orientations.
Inverse Problems 37, 2021.

P Elbau, M Quellmalz, O Scherzer, G Steidl.
Motion detection in diffraction tomography with common circle methods.
Math Comp., 2024. doi:10.1090/mcom/3869